Journal of Computational Physics **152,** 264–280 (1999)
Article ID jcph.1999.6247, available online at http://www.idealibrary.com on IDEAL®

A Chebyshev Spectral Method for Radiative Transfer Equations Applied to Electromagnetic Wave Propagation and Scattering in a Discrete Random Medium

Arnold D. Kim* and Akira Ishimaru†

**Department of Applied Mathematics, Box 352420, University of Washington, Seattle, Washington 98195; and †Department of Electrical Engineering, University of Washington, Seattle, Washington 98195*
E-mail: adkim@amath.washington.edu

Received September 21, 1998; revised February 22, 1999

In this paper, we present a numerical method for solving the radiative transfer equation that models electromagnetic wave propagation in a constant background, plane-parallel medium containing randomly distributed, identically sized, dielectric spheres. Applications of this study include optical waves in media such as biological tissue and fog as well as millimeter waves in rain. In these problems, the scattering is highly anisotropic, which is problematic for standard methods that approximate the integral term of the radiative transfer equation first to yield an associated system of differential equations. In our method, we use a Chebyshev spectral approximation of the spatial part of the 4×1 vector of Stokes parameters. This spectral approximation then yields a coupled, linear system of integral equations that has a bordered, block sparsity structure that can be efficiently solved using a deflated block elimination method. By readjusting the focus of this numerical method to the integral operators instead of the derivative operators, we find that we can effectively study highly anisotropic scattering media. We present some examples of Mie resonant scattering in which a circularly polarized plane wave propagates and scatters in a plane-parallel medium containing randomly distributed, identically sized, dielectric spheres whose radii are comparable to the wavelength.

Key Words: radiative transfer equation; Chebyshev spectral methods; deflated block elimination method; Mie resonance scattering.

1. INTRODUCTION AND SUMMARY

The radiative transfer equation models a radiation field in a medium that scatters, absorbs, and emits radiation [1]. One application of the radiative transfer equation is electromagnetic wave propagation and scattering in a constant background medium containing randomly

0021-9991/99 $30.00

distributed scatterers. This application is useful in engineering studies involving optical waves in biological media, and optical and millimeter wave propagation in rain and fog [2–6], for example. For discrete random media, scattering operations represent the limit of summing the independent scattering events from each of the randomly distributed scatterers. Because the background medium is constant, these problems are spatially uniform. However, a complete analysis of this problem requires the consideration of polarized waves, and therefore, one must solve the polarized radiative transfer equation for the 4×1 vector of Stokes parameters [1–4].

Some common numerical methods for radiative transfer used for this application are the discrete ordinate method [1, 2, 7] and the spherical harmonics method [7]. These methods are very stable and are computationally efficient for scalar problems where the anisotropy of the scattering is small. The finite-element method is a very effective method for studying scalar wave propagation and scattering in highly anisotropic media [8]. However, we have found that these methods are either inefficient or unstable for computing the solution to the polarized problem, especially in highly anisotropic media at large optical depths. Therefore, stable and efficient methods for solving polarized radiative transfer problems are still needed.

This paper addresses the numerical solution of the polarized radiative transfer equation to study electromagnetic wave propagation in plane-parallel geometries containing randomly distributed and highly anisotropic scatterers in a constant background medium. Specifically, we examine a circularly polarized plane wave that is normally incident to the medium. We consider this simple problem first because it is an ideal setting for ascertaining this method's applicability to studying highly anisotropic scattering. We feel that successful applications of this method for more complicated problems can only be done after a thorough investigation of this simplified problem.

Because computational studies of highly anisotropic media require highly resolved angular compenents of the Stokes vector, we have developed a method that allows one to focus attention upon the corresponding integral terms of the radiative transfer equation. In this method, the spatial components of the intensity and the corresponding differential operations are spectrally approximated using Chebyshev polynomials [9]. This spectral approximation yields a system of integral equations for the angularly dependent Chebyshev modes for which one can choose any solution method with which to approximate these scattering operations. Furthermore, this linear system of equations has a bordered, block-banded sparsity structure that can be efficiently solved using a deflated block elimination method [10]. In contrast to Fourier spectral methods for radiative transfer that can only consider periodic boundary conditions [11], Chebyshev methods can consider a variety of boundary conditions [9].

After discussing the governing equations for the aforementioned problem, we present the Chebyshev spectral method. This method yields a coupled system of integral equations for the modes of the Chebyshev expansion. We exploit the sparsity structure of this system by using the deflated block elimination method [10] to solve the discretized version of this linear system of integral equations efficiently. Finally, we examine some computational results of highly anisotropic, Mie resonant scattering where the radii of the dielectric spheres are comparable to the wavelength of the incident radiation [12].

2. THE GOVERNING EQUATIONS

The radiative transfer equation that models electromagnetic wave propagation in a plane-parallel medium (see Fig. 1) containing randomly distributed scatterers in a constant

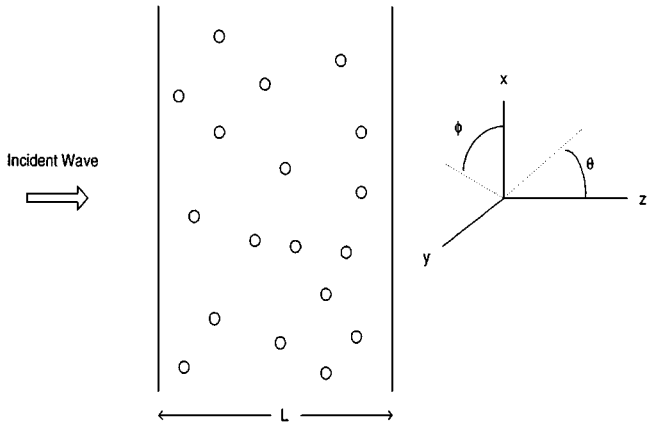

FIG. 1. A sketch of the plane-parallel problem.

background takes the form [3–5]

$$\mu\frac{d\bar{I}(\tau,\mu,\phi)}{d\tau}+\mathcal{T}(\mu,\phi)\bar{I}(\tau,\mu,\phi)$$
$$=\int_0^{2\pi}\int_{-1}^{1}\mathcal{S}(\mu,\phi,\mu',\phi')\bar{I}(\tau,\mu',\phi')\,d\mu'\,d\phi'+\bar{F}(\tau,\mu,\phi), \tag{1}$$

where $\tau=\rho\sigma_t z$ is the optical depth, ρ is the number density of scatterers, σ_t is the total scattering cross section of one of the dielectric spheres, $\mu=\cos\theta$, and $\bar{I}$ is the 4×1 vector of modified Stokes parameters,

$$\bar{I}(\tau,\mu,\phi)=\begin{pmatrix}I_1\\I_2\\U\\V\end{pmatrix}=\begin{pmatrix}\langle E_\theta E_\theta^*\rangle\\\langle E_\phi E_\phi^*\rangle\\2\,\mathrm{Re}\{\langle E_\theta E_\phi^*\rangle\}\\2\,\mathrm{Im}\{\langle E_\theta E_\phi^*\rangle\}\end{pmatrix}. \tag{2}$$

Here, E_θ and E_ϕ are the diffuse electric field components in the $\hat{\theta}$ and $\hat{\phi}$ directions, respectively, Re and Im denote the real and imaginary parts of a complex number, respectively, the asterisk denotes the complex conjugate, and $\langle\cdot\rangle$ denotes an ensemble average.

Consider the expression of the scattered field (far field) from a single dielectric scatterer $(E_\theta^{(s)}, E_\phi^{(s)})$, in terms of the incident field $(E_\theta^{(i)}, E_\phi^{(i)})$,

$$\begin{pmatrix}E_\theta^{(s)}\\E_\phi^{(s)}\end{pmatrix}=\frac{\exp(ikR)}{R}\begin{pmatrix}f_{11}&f_{12}\\f_{21}&f_{22}\end{pmatrix}\begin{pmatrix}E_\theta^{(i)}\\E_\phi^{(i)}\end{pmatrix},$$

where k is the wavenumber, R is the radial distance, and $\{f_{ij}\}$ are the scattering amplitudes. The scattering or Mueller matrix is defined as

$$\mathcal{S}(\mu,\phi,\mu',\phi')$$
$$=\frac{1}{\sigma_t}\begin{pmatrix}f_{11}f_{11}^*&f_{12}f_{12}^*&\mathrm{Re}\{f_{11}f_{12}^*\}&-\mathrm{Im}\{f_{11}f_{12}^*\}\\f_{21}f_{21}^*&f_{22}f_{22}^*&\mathrm{Re}\{f_{21}f_{22}^*\}&-\mathrm{Im}\{f_{21}f_{22}^*\}\\2\,\mathrm{Re}\{f_{11}f_{21}^*\}&2\,\mathrm{Re}\{f_{12}f_{22}^*\}&2\,\mathrm{Re}\{f_{11}f_{22}^*+f_{12}f_{21}^*\}&-\mathrm{Im}\{f_{11}f_{22}^*-f_{12}f_{21}^*\}\\2\,\mathrm{Im}\{f_{11}f_{21}^*\}&2\,\mathrm{Im}\{f_{12}f_{22}^*\}&2\,\mathrm{Im}\{f_{11}f_{22}^*+f_{12}f_{21}^*\}&\mathrm{Re}\{f_{11}f_{22}^*-f_{12}f_{21}^*\}\end{pmatrix}, \tag{3}$$

where the products given in the matrix above are evaluated as $ff^* = f(\mu,\phi)\,f^*(\mu',\phi')$, and the extinction matrix is defined as

$$\mathcal{T}(\mu,\phi) = \begin{pmatrix} 2\,\mathrm{Re}\{M_{11}\} & 0 & \mathrm{Re}\{M_{12}\} & \mathrm{Im}\{M_{12}\} \\ 0 & 2\,\mathrm{Re}\{M_{22}\} & \mathrm{Re}\{M_{21}\} & -\mathrm{Im}\{M_{21}\} \\ 2\,\mathrm{Re}\{M_{21}\} & 2\,\mathrm{Re}\{M_{12}\} & \mathrm{Re}\{M_{11}+M_{22}\} & -\mathrm{Im}\{M_{11}-M_{22}\} \\ -2\,\mathrm{Im}\{M_{21}\} & 2\,\mathrm{Im}\{M_{12}\} & \mathrm{Im}\{M_{11}-M_{22}\} & \mathrm{Re}\{M_{11}+M_{22}\} \end{pmatrix}, \quad (4)$$

where

$$\begin{pmatrix} M_{11} & M_{12} \\ M_{21} & M_{22} \end{pmatrix} = i\frac{2\pi}{k\sigma_t}\begin{pmatrix} f_{11} & f_{12} \\ f_{21} & f_{22} \end{pmatrix}.$$

For spherical scatterers, the Mie scattering solution [12, 13] provides the exact values of the scattering amplitudes $\{f_{11},\ f_{12},\ f_{21},\ f_{22}\}$ given the radius of the sphere, wavelength of the incident wave, and relative refractive index of the sphere to the background. In addition, due to the axial symmetry of the spherical scatterers, the extinction matrix becomes diagonal because of the following properties of M for spherical particles [3]:

$$M_{11} = M_{22}, \qquad M_{12} = M_{21} = 0.$$

For our computations, only a normally incident, circularly polarized plane wave illuminates the medium. This plane wave manifests itself in the source term as

$$\bar{F}(\tau,\mu,\phi) = \mathcal{S}(\mu,\phi,\mu'=1,\phi'=0)\begin{pmatrix} 1/2 \\ 1/2 \\ 0 \\ \pm 1 \end{pmatrix}\exp(-\tau), \quad (5)$$

where $\pm$ denotes a right-handed or left-handed circular polarization, respectively. Therefore, assuming that there is no other intensity directed into the medium, $0 \le \tau \le \tau_o$ gives the boundary conditions,

$$\begin{aligned} \bar{I}(\tau=0,\mu) &= 0 \qquad \text{for } 0 < \mu \le 1, \\ \bar{I}(\tau=\tau_o,\mu) &= 0 \qquad \text{for } -1 \le \mu < 0. \end{aligned} \quad (6)$$

To treat the azimuthal dependence of the intensity vector in (1), we consider a Fourier expansion of the Stokes vector,

$$\bar{I}(\tau,\mu,\phi) = \sum_{n=-\infty}^{\infty} \bar{I}^{(n)}(\tau,\mu)\exp(in\theta). \quad (7)$$

Notice that the source term defined in (5) does not depend on θ, and thus, only the mode-zero component of the Fourier expansion above, $\bar{I}^{(0)}(\tau,\mu)$ is needed to solve the problem. By carrying out the analysis of this Fourier expansion in (1), we obtain

$$\mu\frac{d}{d\tau}\bar{\mathcal{I}}_1(\tau,\mu) = -\bar{\mathcal{I}}_1(\tau,\mu) + \int_{-1}^{1} K_1(\mu,\mu')\bar{\mathcal{I}}_1(\tau,\mu')\,d\mu' + \bar{F}_1(\mu)\exp(-\tau) \quad (8)$$

$$\mu\frac{d}{d\tau}\bar{\mathcal{I}}_2(\tau,\mu) = -\bar{\mathcal{I}}_2(\tau,\mu) + \int_{-1}^{1} K_2(\mu,\mu')\bar{\mathcal{I}}_2(\tau,\mu')\,d\mu' + \bar{F}_2(\mu)\exp(-\tau), \quad (9)$$

where

$$\bar{\mathcal{I}}_1 = \begin{pmatrix} I_1^{(0)} \\ I_2^{(0)} \end{pmatrix} \quad \text{and} \quad \bar{\mathcal{I}}_2 = \begin{pmatrix} U^{(0)} \\ V^{(0)} \end{pmatrix} \tag{10}$$

are vectors containing the mode-zero components of the Fourier series of modified Stokes parameters with respect to the azimuthal angle, and

$$K_1(\mu, \mu') = \int_0^{2\pi} S_1(\mu, \mu', \phi - \phi')\, d(\phi - \phi') \tag{11}$$

$$K_2(\mu, \mu') = \int_0^{2\pi} S_4(\mu, \mu', \phi - \phi')\, d(\phi - \phi') \tag{12}$$

are the kernels of the integral operators. Here S_1 and S_4 are the submatrices of the Mueller matrix, (3), when it is written as

$$\mathcal{S} = \begin{pmatrix} S_1 & S_2 \\ S_3 & S_4 \end{pmatrix}.$$

The source terms, $\bar{F}_1$ and $\bar{F}_2$, are the mode-zero components of the source term given in (5). A complete derivation of this reduced system can be found in [5].

3. THE SOLUTION METHOD

3.1. *The Chebyshev Spectral Method*

In this section, we present the Chebyshev spectral method. For simplicity of notation, we present this method for scalar problems, since the extension of this method for the polarized problem defined in the previous section is intuitive. First, consider mapping the spatial domain from $0 \le \tau \le \tau_o$ to $-1 \le s \le 1$ by the linear transformation, $s = 2\tau/\tau_o - 1$. Then the equation of transfer takes the form

$$2\mu \frac{dI(s, \mu)}{ds} + \tau_o I(s, \mu) = \tau_o \int_{-1}^{1} K(\mu, \mu') I(s, \mu')\, d\mu' + \tau_o F(\mu) \exp(-\tau_o(s+1)/2). \tag{13}$$

Now we consider the spectral approximation of the intensity,

$$I(s, \mu) = \sum_{k=0}^{\infty} \hat{a}_k(\mu) T_k(s) \cong \sum_{k=0}^{N} \hat{a}_k(\mu) T_k(s), \tag{14}$$

where $\{T_k(s)\}$ is the complete and orthonormal set of Chebyshev polynomials,

$$T_k(s) = \cos[k \cos^{-1}(s)]. \tag{15}$$

By evaluating the Chebyshev polynomials at the collocation points, $s_j = \cos(\pi j/N)$ for $j = 0, \ldots, N$, we can also write the derivative in terms of an expansion of Chebyshev polynomials [9],

$$\frac{dI(s, \mu)}{ds} \cong \sum_{k=1}^{N} \hat{a}_k^{(1)}(\mu) T_k(s), \tag{16}$$

where $\{\hat{a}_k^{(1)}(\mu)\}$ is related to $\{\hat{a}_k(\mu)\}$ through the recursion relation,

$$\hat{a}_k(\mu) = \frac{1}{2k}\left[c_{k-1}\hat{a}_{k-1}^{(1)}(\mu) - \hat{a}_{k+1}^{(1)}(\mu)\right] \qquad \text{for } k = 1, 2, \ldots, N \tag{17}$$

with

$$c_k = \begin{cases} 2 & \text{for } k = 0, N \\ 1 & \text{for } 1 \le k \le N-1. \end{cases} \tag{18}$$

We can also write the exponential part of the source term in a Chebyshev expansion,

$$\exp(-\tau_o(s+1)/2) \cong \sum_{k=0}^{N} \hat{b}_k T_k(s). \tag{19}$$

Substituting these expansions into (13) and using the orthogonality of Chebyshev polynomials,

$$\frac{2}{\pi c_k}\int_{-1}^{1} T_j(s)T_k(s)\frac{ds}{\sqrt{1-s^2}} = \begin{cases} 1 & \text{for } j = k \\ 0 & \text{for } j \ne k, \end{cases} \tag{20}$$

we obtain

$$2\mu\hat{a}_k^{(1)}(\mu) + \tau_o\hat{a}_k(\mu) = \tau_o\mathcal{K}\hat{a}_k(\mu) + \tau_o\hat{b}_k f(\mu), \tag{21}$$

where

$$\mathcal{K}\hat{a}_k(\mu) = \int_{-1}^{1} K(\mu, \mu')\hat{a}_k(\mu')\, d\mu'.$$

The derivative operation is poorly conditioned in Chebyshev transform space [9, 14], but we can avoid explicit derivative operations by transforming (21) into a coupled system of integral equations for $\{\hat{a}_k^{(1)}(\mu)\}$. Using (17) on (21), one obtains

$$\begin{aligned} 2\mu\hat{a}_0^{(1)}(\mu) + \mathcal{L}_1\hat{a}_0(\mu) &= \tau_o\hat{b}_0 f(\mu) && \text{for } k = 0 \\ 2\mu\hat{a}_k^{(1)}(\mu) + c_{k-1}\mathcal{L}_{2k}\hat{a}_{k-1}^{(1)}(\mu) - \mathcal{L}_{2k}\hat{a}_{k+1}^{(1)}(\mu) &= \tau_o\hat{b}_k f(\mu) && \text{for } 1 \le k \le N-1 \\ 2\mu\hat{a}_N^{(1)}(\mu) + c_{N-1}\mathcal{L}_{2N}\hat{a}_{N-1}^{(1)}(\mu) &= \tau_o\hat{b}_N f(\mu) && \text{for } k = N, \end{aligned} \tag{22}$$

where

$$\mathcal{L}_j = \frac{\tau_o}{j}(\mathcal{I} - \mathcal{K}), \tag{23}$$

and $\mathcal{I}$ is the identity operator.

Since $T_k(\pm 1) = (\pm 1)^k$, the boundary conditions are written in Chebyshev transform space as

$$I(s = -1, \mu) = \sum_{k=0}^{N}(-1)^k\hat{a}_k(\mu) = 0 \qquad \text{for } 0 < \mu \le 1. \tag{24}$$

$$I(s = +1, \mu) = \sum_{k=0}^{N}\hat{a}_k(\mu) = 0 \qquad \text{for } -1 \le \mu < 0. \tag{25}$$

Applying (17) to the boundary conditions defined above yields

$$\hat{a}_0(\mu) - \hat{a}_0^{(1)}(\mu) + \frac{1}{4}\hat{a}_1^{(1)}(\mu) + \sum_{k=2}^{N-1} \frac{(-1)^{k+1}}{2}\left(\frac{1}{k+1} - \frac{1}{k-1}\right)\hat{a}_k^{(1)}(\mu) + \frac{1}{2(N-1)}\hat{a}_N^{(1)}(\mu) = 0 \tag{26}$$

for $0 < \mu \leq 1$, and

$$\hat{a}_0(\mu) + \hat{a}_0^{(1)}(\mu) + \frac{1}{4}\hat{a}_1^{(1)}(\mu) + \sum_{k=2}^{N-1} \frac{1}{2}\left(\frac{1}{k+1} - \frac{1}{k-1}\right)\hat{a}_k^{(1)}(\mu) - \frac{1}{2(N-1)}\hat{a}_N^{(1)}(\mu) = 0 \tag{27}$$

for $-1 \leq \mu < 0$. We now have $N+2$ equations for the $N+2$ unknowns, $\{\hat{a}_0(\mu), \hat{a}_0^{(1)}(\mu), \ldots, \hat{a}_N^{(1)}(\mu)\}$.

3.2. *The Deflated Block Elimination Method*

If we write the unknown modes of the system of integral equations defined above as a vector,

$$X^T = \begin{pmatrix} \hat{a}_0^{(1)}(\mu) & \hat{a}_1^{(1)}(\mu) & \cdots & \hat{a}_N^{(1)}(\mu) & \hat{a}_0(\mu) \end{pmatrix}, \tag{28}$$

then this system defined by (22) with the boundary equations, (26) and (27), can be written as

$$MX = F. \tag{29}$$

The right hand side vector is

$$F^T = \tau_o \begin{pmatrix} \hat{b}_0 f(\mu) & \hat{b}_1 f(\mu) & \cdots & \hat{b}_N f(\mu) & 0 \end{pmatrix}. \tag{30}$$

The $(N+2) \times (N+2)$ matrix of operators is

$$M = \begin{pmatrix} A & B \\ C^T & D \end{pmatrix}, \tag{31}$$

where A is an $(N+1) \times (N+1)$ tridiagonal matrix of operators,

$$A = \begin{pmatrix} 2\mu\mathcal{I} & 0 & & & & \\ \mathcal{L}_1 & 2\mu\mathcal{I} & -\mathcal{L}_2 & & & \\ & \mathcal{L}_4 & 2\mu\mathcal{I} & -\mathcal{L}_4 & & \\ & & \ddots & \ddots & \ddots & \\ & & & \mathcal{L}_{2(N-1)} & -2\mu\mathcal{I} & \mathcal{L}_{2(N-1)} \\ & & & & \mathcal{L}_{2N} & 2\mu\mathcal{I} \end{pmatrix}, \tag{32}$$

B is an $(N+1)\times 1$ matrix corresponding to operations on $\hat{a}_0(\mu)$,

$$B = \begin{pmatrix} \mathcal{L}_1 \\ 0 \\ \vdots \\ 0 \end{pmatrix}, \tag{33}$$

C^T is a $1\times(N+1)$ matrix containing the operations associated to the boundary conditions that act upon $\{\hat{a}_k^{(1)}(\mu)\}$,

$$C^T = \begin{pmatrix} \mathcal{I}^{\pm} & \frac{1}{4}\mathcal{I} & -\frac{1}{3}\mathcal{I}^{\pm} & \cdots & -\frac{1}{2(N-1)}\mathcal{I}^{\pm} \end{pmatrix}, \tag{34}$$

and $D=\mathcal{I}$ is the identity operator associated to the boundary conditions that acts upon $\hat{a}_0(\mu)$. Here, we define

$$\mathcal{I}^{\pm} = \begin{cases} \mathcal{I} & \text{for } \mu < 0 \\ -\mathcal{I} & \text{for } \mu > 0. \end{cases} \tag{35}$$

Notice that the matrix, A, has a tridiagonal sparsity structure, and that the off-diagonal operations are the same modulo a scalar factor. In addition, the B, C^T, and D matrices lie on the "border" of the A matrix, and thus, we have a bordered, tridiagonal system of operators.

At this stage in the method, one can choose any numerical treatment of the integral operators including Nyström methods and expansion methods [15]. Since this spectral method treats the spatial part of the radiative transfer equation, we can refocus our attention to the scattering operators. This idea is very advantageous for studies of highly anisotropic scattering since the corresponding integral operations require highly resolved numerical approximations. Let us assume that we have chosen a particular method by which to solve the integral equation yielding a discretized version of the system above. The system then becomes a block tridiagonal, linear system of equations.

The deflated block elimination method is a direct solution method which allows one to consider the block tridiagonal part of the system separately. Thus, a modified Gaussian elimination algorithm for block tridiagonal systems can be used to greatly reduce the amount of storage and work necessary to solve (29). To use the deflated block elimination method, let us define

$$x^T = \begin{pmatrix} \hat{a}_0^{(1)}(\mu) & \hat{a}_1^{(1)}(\mu) & \cdots & \hat{a}_N^{(1)}(\mu) \end{pmatrix}, \qquad y = (\hat{a}_0(\mu)),$$

and

$$f^T = \tau_o(\hat{b}_0 f(\mu) \quad \hat{b}_1 f(\mu) \quad \cdots \quad \hat{b}_N f(\mu)), \qquad g = (0).$$

Then,

$$MX = \begin{pmatrix} A & B \\ C^T & D \end{pmatrix}\begin{pmatrix} x \\ y \end{pmatrix} = \begin{pmatrix} f \\ g \end{pmatrix}, \tag{36}$$

and the generalized, deflated block algorithm

1. Solve $AW = B$
2. Solve $Aw = f$
3. Compute $S = D - C^T W$ (the Schur compliment)
4. Solve $Sy = g - C^T w$
5. Compute $x = w - Wy$

can be used to solve the system of linear equations given in (29) efficiently.

The storage requirements needed to perform this algorithm are very small. Let us assume that one chooses a discretization of the integral equations that yields $q \times q$ matrices for each operation given in matrix A. The diagonal blocks of A will be diagonal matrices themselves, and the off-diagonal matrices in A only differ from each other by a constant factor, τ_o/j, as seen in the definition given in (23). Therefore, only a $q \times 1$ vector containing the diagonal elements of the matrix that approximates $2\mu\mathcal{I}$ and the $q \times q$ matrix that approximates $\mathcal{L}_1$ is needed to "effectively" store the entire A matrix in a sparse solver for the block tridiagonal system of equations.

In addition to reducing storage requirements, the diagonal structure of the diagonal blocks of A slightly reduces the work necessary to solve the associated block tridiagonal systems given in steps 1 and 2 in the algorithm above. Furthermore, the diagonal structure of the blocks in C^T can be exploited in steps 3 and 4 of the algorithm above to reduce the work and storage necessary to multiply C^T to W and w. If one uses $N + 1$ Chebyshev modes where N is the highest Chebyshev mode used in the spectral approximation, (14), then a conservative estimate of the work required to perform the entire deflated block elimination method given above is approximately $q^3(N - 1)$ to leading order.

It is noteworthy that throughout this section, we have presented the Chebyshev spectral method in terms of the scalar problem for notational simplicity. For the polarized problem, the value of q corresponds to the total number of discretized elements for all of the Stokes parameters (I_1, I_2, U, and V) in the Stokes vector, and not to the number of discrete points or modes used to approximate each of the Chebyshev coefficients, $\hat{a}_k(\mu)$. For example, if we use a $\tilde{q}$-point quadrature rule in a Nyström method to solve the integral equations for the 4×1 Stokes vector, then $q = 4\tilde{q}$ as long as we resolve each Stokes parameter in the same way.

4. NUMERICAL RESULTS: MIE RESONANT SCATTERING

Much of the current interest in multiple scattering in random media comes from the investigation of localization of classical waves [16]. One particular aspect of this research involves the study of electromagnetic wave scattering from randomly distributed, dielectric spheres in the Mie resonance regime where the diameters of the spheres are comparable to the wavelength [17, 18]. To the authors' knowledge, a thorough numerical investigation of the radiative transfer equation in the Mie resonance regime has not been carried out, even for planar geometries, since with standard methods it is difficult to resolve the angular components of the intensity while solving the associated boundary value problem stably. We present here, as an example of the Chebyshev spectral method, some computations of a continuous, circularly polarized, plane wave incident upon a plane-parallel medium of dielectric spheres tuned to Mie resonance.

For our computations, we used a Nyström method [15] to solve the system of integral equations that employed the abcissa and weights of the Legendre polynomials for the

Gaussian quadrature rule. This method was chosen for its ease of implementation as well as its ability to investigate anisotropic media for these test problems. An algorithm that computed the Mie scattering solution presented in [13] was used to calculate the elements of the Mueller matrix, (3), and the integrals, (11) and (12), were computed using numerical quadrature.

To examine the numerical results of this method, we computed the left-handed and right-handed circularly polarized (LHC and RHC, respectively) transmitted and reflected diffuse intensities,

$$I_{\mathrm{LHC}}^{(t)}(\mu) = \tfrac{1}{2}[I_1(\tau = \tau_o, \mu) + I_2(\tau = \tau_o, \mu) + V(\tau = \tau_o, \mu)], \tag{37}$$

$$I_{\mathrm{LHC}}^{(r)}(\mu) = \tfrac{1}{2}[I_1(\tau = 0, \mu) + I_2(\tau = 0, \mu) + V(\tau = 0, \mu)], \tag{38}$$

$$I_{\mathrm{RHC}}^{(t)}(\mu) = \tfrac{1}{2}[I_1(\tau = \tau_o, \mu) + I_2(\tau = \tau_o, \mu) - V(\tau = \tau_o, \mu)], \tag{39}$$

$$I_{\mathrm{RHC}}^{(r)}(\mu) = \tfrac{1}{2}[I_1(\tau = 0, \mu) + I_2(\tau = 0, \mu) - V(\tau = 0, \mu)]. \tag{40}$$

In addition, we examined the magnitudes of the LHC and RHC transmitted and reflected fluxes,

$$\mathcal{F}_{\mathrm{LHC}}^{(t)} = 2\pi \int_{-1}^{1} I_{\mathrm{LHC}}^{(t)}(\mu)\mu \, d\mu, \tag{41}$$

$$\mathcal{F}_{\mathrm{LHC}}^{(r)} = 2\pi \int_{-1}^{1} I_{\mathrm{LHC}}^{(r)}(\mu)\mu \, d\mu, \tag{42}$$

$$\mathcal{F}_{\mathrm{RHC}}^{(t)} = 2\pi \int_{-1}^{1} I_{\mathrm{RHC}}^{(t)}(\mu)\mu \, d\mu, \tag{43}$$

$$\mathcal{F}_{\mathrm{RHC}}^{(r)} = 2\pi \int_{-1}^{1} I_{\mathrm{RHC}}^{(r)}(\mu)\mu \, d\mu. \tag{44}$$

These flux integrals were computed using the Gaussian quadrature rule associated with the aforementioned Nyström method.

4.1. *Scattering within and outside of the Mie Resonance Regime*

In order to demonstrate the need for highly resolved integral operations for these computations, we performed some computations to compare scattering within and outside of the Mie resonance regime. In Fig. 2, the angular distribution of the scattered intensity in the far field regime from a single dielectric sphere (the scattering diagram) is plotted to show the necessity for highly resolved numerical approximations of the integral operators for Mie resonant scattering. The scattering diagram is directly computed from the Mie scattering solution [12]. In Fig. 3, the transmitted and reflected intensities were computed to show the differences between the nearly isotropic and anisotropic scattering. To examine scattering within the Mie resonance regime, we considered an incident plane wave of wavelength $\lambda = 3$ mm and dielectric spheres of radii of $a = 3$ mm. For the cases outside of the Mie resonance regime, we considered wavelengths of $\lambda = 30$ mm on the same dielectric spheres.

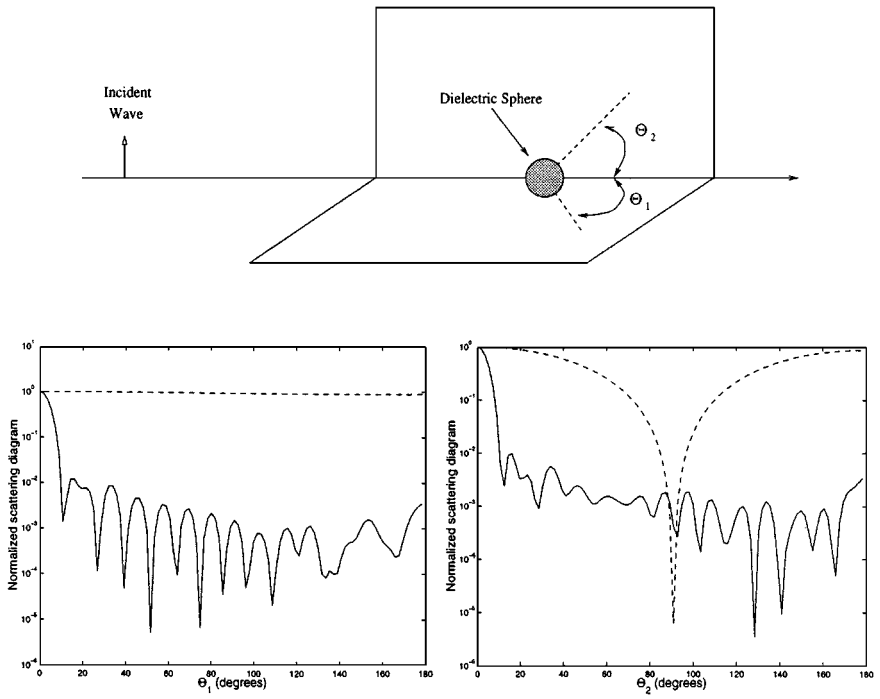

FIG. 2. Angular distributions of the far field scattered intensity (scattering diagram) for a single dielectric sphere at two different frequencies. The left plot shows the scattering diagram on the plane orthogonal to the incident polarization, and the right plot shows the scattering diagram on the plane parallel to the incident polarization. The solid line represents the case in which the wavelength is comparable to the diameter of the sphere and the dashed line represents the case in which the wavelength is significantly larger ($\sim 10\times$) than the diameter of the sphere.

4.2. *Conservative Scattering*

Conservative scattering refers to the case in which there is no absorption in the medium (the relative refractive index of the scatterers, n_{rel} is a strictly real number). Then all of the power is scattered and the total flux transmitted and reflected out of the medium is equal to the incident power [2]. We used conservative scattering to test the Chebyshev spectral method's ability to solve the polarimetric radiative transfer equation. A sample of the results from these computations can be found in Table I. Here, we considered highly anisotropic

TABLE I
Relative Error of the Conservation of Flux for Various Numbers of Chebyshev Modes and Quadrature Points

Number of Chebyshev modes	Number of quadrature points		
	20	40	60
5	0.16607E-1	0.16607E-1	0.16607E-1
9	0.91983E-5	0.91983E-5	0.91983E-5
17	0.86012E-10	0.48853E-10	0.35104E-10
33	0.85963E-10	0.48802E-10	0.35055E-10
65	0.85963E-10	0.48802E-10	0.35054E-10

Note. Here $\tau_o = 5.0$, $a = 3$ mm, $\lambda = 3$ mm, and $n_{\text{rel}} = 2.15$.

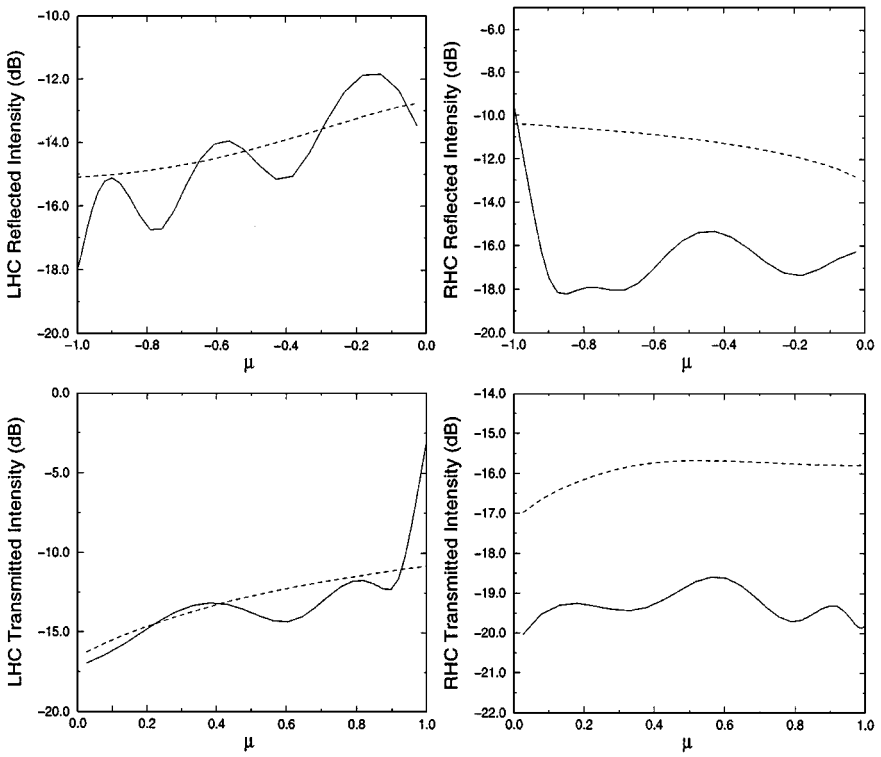

FIG. 3. Comparison of intensity computations within and outside of the Mie resonance regime. Here we have plotted the LHC and RHC polarized, transmitted, and reflected intensities. The solid lines correspond to the case $a = \lambda = 3$ mm (within the Mie resonance regime) and the dashed lines correspond to the case $a = 3$ mm and $\lambda = 30$ mm (outside the Mie resonance regime). For these computations, $\tau_o = 2.0$, $n_{\text{rel}} = 2.15 + i0.01$, the number of Chebyshev modes was fixed at 65, and the number of quadrature points was fixed at 60.

scattering where the wavelength of the incident radiation, λ, and the radius of the spheres, a, were equal to 3 mm for a moderate optical depth of $\tau_o = 5.0$. From these results, we observed that the method demonstrated the typical hyper-algebraic convergence of spectral methods with the conservation of power calculation as the number of Chebyshev modes increased. Furthermore, as the number of quadrature points increased, we observed that the error decreased. In Fig. 4, we show a sample result of our computations for various resolutions of the Nyström method. Notice that the scattering for the computations shown in Fig. 4, however, is not conservative. The relative refractive index of the scatterers in that plot is $n_{\text{rel}} = 2.15 + i0.01$. Therefore, there is some absorption in the medium. The radius, wavelength, and relative refractive index values correspond to the experimental configuration presented in [17].

It is noteworthy that in Table I, the error converges to some finite value as one resolves the Chebyshev spectrum. Because the associated system of integral equations is solved using a Nyström method that has some inherent error properties, the spectral resolution of the conservation calculation is limited. In addition, we conjecture that, as one resolves the integral operations by increasing the quadrature points, the condition number of the matrix, M, increases and thereby limits the accuracy of the method, slightly. However, relative errors on the order of 10^{-10} for these conservation calculations is negligibly small,

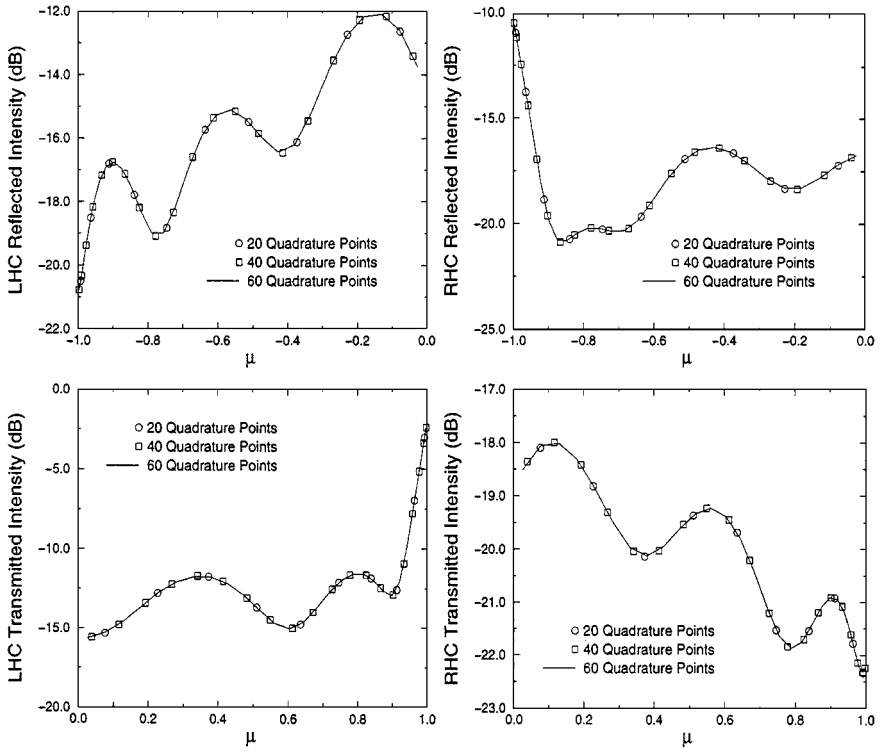

FIG. 4. Numerical quadrature refinement studies. Here we have plotted the LHC and RHC polarized, transmitted, and reflected intensities for a variety of angular resolutions. For these computations, $\tau_o = 1.0$, $a = 3$ mm, $\lambda = 3$ mm, $n_{\text{rel}} = 2.15 + i0.01$, and the number of Chebyshev modes was fixed at 17.

and indicates that the Chebyshev spectral method is very effective for these conservative scattering computations.

4.3. *Boundary Conditions*

From our observations, we have determined that under-resolving the Chebyshev expansion, (14), manifests itself in the results of these computations as errors in satisfying the boundary conditions, (26) and (27). The original problem states that no intensity was directed in toward the medium, and so both the LHC and RHC components of the intensity must satisfy

$$I_{\text{L/RHC}}(\tau = 0, \mu) = 0 \qquad \text{for } 0 < \mu \leq 1, \tag{45}$$

$$I_{\text{L/RHC}}(\tau = \tau_o, \mu) = 0 \qquad \text{for } -1 \leq \mu < 0. \tag{46}$$

Therefore, we computed the infinity norm of the error at the boundaries, ϵ^{BC}, defined as

$$\epsilon^{BC} = \| I^{\text{computed}} - I^{\text{true}} \|_{\infty}, \tag{47}$$

which gives the maximum difference error associated with the boundary data for the LHC and RHC components of the transmitted and reflected intensities as a means of studying the

TABLE II
Infinity Norm of the Error Corresponding to the Boundary Conditions, ϵ^{BC}, for Various Numbers of Chebyshev Modes

Number of Chebyshev modes	Reflected intensity		Transmitted intensity	
	LHC	RHC	LHC	RHC
9	0.1039E-1	0.8859E-2	0.3039E-1	0.2592E-1
17	0.7030E-3	0.6000E-3	0.2532E-4	0.2444E-4
33	0.5648E-5	0.4743E-5	0.1527E-6	0.1481E-6
65	0.4377E-11	0.3415E-11	0.1148E-12	0.1080E-12
129	0.2998E-15	0.3977E-15	0.3863E-15	0.2769E-15

Note. Here $\tau_o = 10.0$, $a = 3$ mm, $\lambda = 3$ mm, $n_{\text{rel}} = 2.15 + i0.01$, and the number of quadrature points was fixed at 40.

convergence of the Chebyshev spectral method. A sample of the results is found in Table II. For these computations, we considered an optical depth of $\tau_o = 10.0$ for $a = \lambda = 3$ mm, and $n_{\text{rel}} = 2.15 + i0.01$. The number of quadrature points remained fixed at 40 and we varied the number of Chebyshev modes. Again, we observed that increasing the number of Chebyshev modes indicates the spectral accuracy of this method. The boundary error reduces hyper-algebraically as the number of modes increases. Therefore, the resolution of the Chebyshev expansion affects the method's ability to satisfy the boundary conditions.

4.4. *First Order Scattering*

If we consider a tenuous distribution of the dielectric spheres, then the optical depth becomes small, $\tau_o \ll 1$, and the first order scattering approximation is valid [2]. The first order scattering solution assumes that total radiation incident upon the scatterers is approximately the incident radiation. We compared the computed solutions to the first order scattering approximation at small optical depths in the Mie resonance regime to examine the consistency of the Chebyshev spectral method. In these comparison studies, we found that the computed solutions agree very well with the first order scattering approximation.

A sample comparison can be seen in Fig. 5. For this computation, we considered an optical depth of $\tau_o = 0.05$ with $a = \lambda = 3$ mm, and $n_{\text{rel}} = 2.15 + i0.10$. Notice that for this computation, the absorption is a little larger than that from the previous computations presented above. The computed solution qualitatively agrees very well with the first order scattering solution. Quantitative differences are greatest as $\mu \approx 0$. Because the abscissas of the Legendre polynomials are unevenly spaced and clustered near the boundaries at $\mu = \pm 1$, the intensities have the lowest angular resolution at $\mu \approx 0$. Another quadrature rule may provide a better resolution at points near $\mu = 0$, but since the distribution of scattered intensity in the Mie resonance regime is directed in the "forward" direction, $\cos\theta = \mu = 1$ (see Fig. 2), the higher angular resolution due to the locations of the Legendre abscissa at $\mu \approx 1$ is more appropriate for these problems. From this example and other numerical studies that we have done, we observed that the computed solution from the Chebyshev spectral method is consistent with the first order scattering approximation within the approximation's asymptotic region of validity.

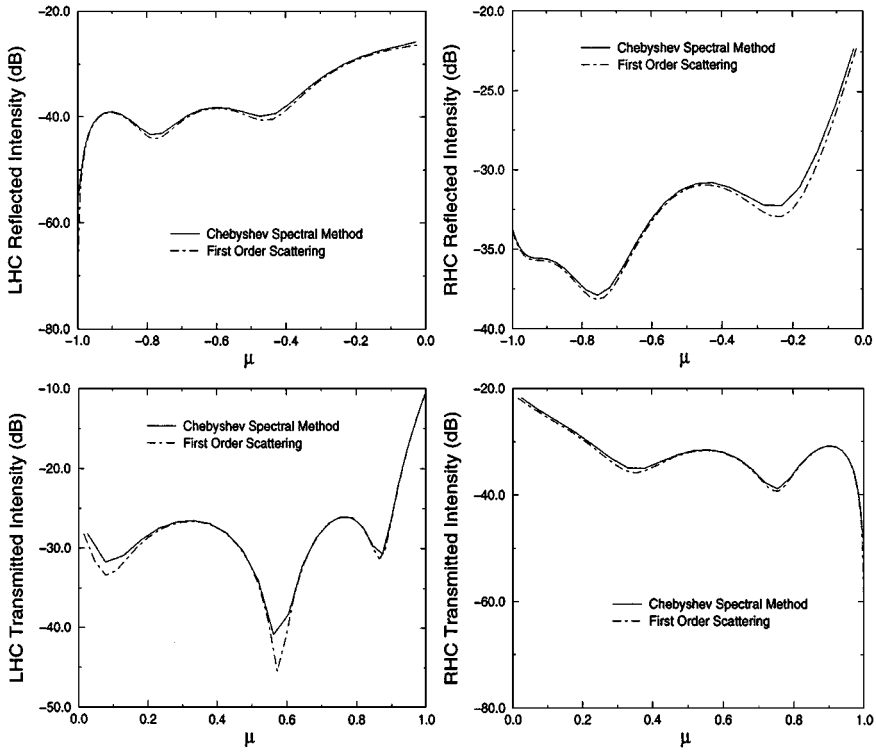

FIG. 5. A comparison of the Chebyshev spectral method's computed solution and the first order scattering approximation solution. Here $\tau_o = 0.05$, $a = \lambda = 3$ mm, and $n_{\text{rel}} = 2.15 + i0.10$. For these computed solutions, we used 60 quadrature points and the number of Chebyshev modes was 33.

5. CONCLUSION

We have discussed a Chebyshev spectral method for solving the polarized radiative transport equation in a plane-parallel, spatially homogeneous medium that models electromagnetic wave propagation and scattering from a discrete random medium. This method differs from other methods for radiative transfer by using a Chebyshev spectral expansion for the spatial part of the intensity vector, thereby yielding a coupled system of Fredholm integral equations of the second kind. In this paper, we used a Nyström method to solve the integral equations, but the Chebyshev spectral method does not restrict one to any particular numerical integral equation method. The bordered, block tridiagonal system of equations that results from the spectral approximation can be efficiently solved using a deflated block elimination method in conjunction with a block tridiagonal Gaussian elimination algorithm. By refocusing our attention to the integral operations rather than the derivative operations, we are able to examine highly anisotropic scattering media, including Mie resonant media. By examining conservative scattering, errors associated with the boundary conditions, and comparisons with first order scattering for problems in the Mie resonance regime, we have demonstrated the Chebyshev spectral method's effectiveness for solving highly anisotropic scattering problems.

The two-frequency radiative transfer equation governs electromagnetic pulse propagation in discrete random media [19]. For these pulse problems, the intensity vector parametrically depends on two frequencies and is, in general, a complex function. Computational methods

for two-frequency radiative transfer involve solving radiative transfer equations for each frequency pair to construct the two-frequency spectrum of the intensity which is recovered into the time domain by Fourier transforms [6]. The frequency dependent problem, therefore, requires an efficient method for computing the solution to the radiative transfer equation for a given frequency pair. Therefore, the method presented in this paper for continuous waves can be used as the solver for the associated radiative transfer equations for each frequency pair to generate a two-frequency spectrum.

This method was designed with the specific intent of studying polarimetric problems with highly anisotropic scattering from discrete random media. The advantage of this method is that it allows one to focus direct attention on resolving the integral operations instead of the boundary value problem. However, there are potential extensions of this method for other problems of radiative transfer. As previously mentioned in the Introduction, Chebyshev spectral methods can solve a wide variety of boundary value problems—Dirichlet, Neumann, and Robin boundary conditions [9]—and may be an attractive alternative to existing Fourier methods [11] that can only solve periodic boundary value problems. The Chebyshev spectral method should be general enough to consider spatially varying opacities and higher spatial dimensions in a way similar to that presented in [11], although we have not investigated this idea thoroughly. We will be considering more complicated geometries in future studies, during which we will ascertain this method's usefulness for larger spatial dimensional problems. In preparation for these problems, we are currently investigating the effectiveness of iterative methods in solving the linear system of integral equations to increase the performance and decrease storage requirements further.

ACKNOWLEDGMENTS

The authors express their gratitude to Dominick Obrist and Peter J. Schmid for their thoughtful discussions and help in developing the method. In addition, we thank Randall J. LeVeque for his help in composing the manuscript. The work was supported by the National Science Foundation, the Office of Naval Research, and the Army Research Office.

REFERENCES

1. S. Chandrasekhar, *Radiative Transfer* (Dover, New York, 1960).
2. A. Ishimaru, *Wave Propagation and Scattering in Random Media* (IEEE Press, New York, 1997).
3. A. Ishimaru and R. Cheung, Multiple scattering effects on wave propagation due to rain, *Ann. Télécommun.* **35** (1980).
4. R. Cheung and A. Ishimaru, Transmission, backscattering, and depolarization of waves in randomly distributed spherical particles, *Appl. Opt.* **21**(20), 3792 (1982).
5. R. Cheung, *Millimeter and Optical Waves in Rain and Fog*, Ph.D. thesis, University of Washington, Seattle, WA, 1981.
6. A. D. Kim and A. Ishimaru, Optical diffusion of continuous-wave, pulsed, and density waves in scattering media and comparisons with radiative transfer, *Appl. Opt.* **37**(22), 5313 (1998).
7. J. Lenoble (Ed.), *Radiative Transfer in Scattering and Absorbing Atmospheres: Standard Computational Procedures* (Deepak Publishing, Hampton, VA 1985).
8. V. B. Kisselev, L. Roberti, and G. Perona, An application of the finite-element method to the solution of the radiative transfer equation, *J. Quant. Spectrosc. Radiat. Transfer* **51**(4), 603 (1994).
9. C. Canuto, M. Y. Hussaini, A. Quarteroni, and T. A. Zang, *Spectral Methods in Fluid Dynamics* (Springer-Verlag, Berlin/New York, 1988).

10. T. F. Chan and D. C. Resasco, Generalized deflated block-elimination, *SIAM J. Numer. Anal.* **23**(5), 913 (1986).
11. B. Ritchie, P. G. Dykema, and D. Braddy, Use of fast-Fourier-transform computational methods in radiation transport, *Phys. Rev. E* **56**, 2217 (1997).
12. M. Kerker, *The Scattering of Light and Other Electromagnetic Radiation* (Academic Press, New York, 1969).
13. C. F. Bohren and D. R. Huffman, *Absorption and Scattering of Light by Small Particles* (Wiley, New York, 1983).
14. A. Lundblah, D. S. Henningson, and A. V. Johansson, *An Efficient Spectral Integration Method For the Solution of the Navier–Stokes Equations*, Technical Report, The Aeronautical Research Institute of Sweden, 1992.
15. L. M. Delves and J. L. Mohamed, *Computational Methods for Integral Equations* (Cambridge Univ. Press, Cambridge, UK, 1985).
16. D. S. Wiersma, P. Bartonlini, A. Lagendijk, and R. Righini, Localization of light in a disordered medium, *Nature* **390**, 671 (1997).
17. Y. Kuga, A. Ishimaru, and D. Rice, Velocity of coherent and incoherent electromagentic waves in a dense strongly scattering medium, *Phys. Rev. B* **48**(17), 13155 (1993).
18. Y. N. Barabenenkov and M. Y. Barabenenkov, Radiative transfer theory with time delay for the effect of pulse entrapping in a resonant medium: General transfer equation and point-like scatterer model, *Waves in Random Media* **7**, 607 (1997).
19. A. Ishimaru, Diffusion of a pulse in densely distributed scatterers, *J. Opt. Soc. Am.* **68**, 1045 (1978).